Energy-based nonlinear control of hydraulically actuated pitch-servo systems

Henriksen, Lars Christian; Poulsen, Niels Kjølstad

Published in:
EWEC 2009 Proceedings online

Publication date:
2009

Document Version
Publisher's PDF, also known as Version of record

Energy-based Nonlinear Control of Hydraulically Actuated Pitch-Servo Systems

L. C. Henriksen
Risø National Laboratory for Sustainable Energy
Technical University of Denmark
DK-4000 Roskilde, Denmark
larh@risoe.dtu.dk

N. K. Poulsen
Dept. of Informatics and Mathematical Modelling
Technical University of Denmark
DK-2800 Kgs. Lyngby, Denmark
nkp@imm.dtu.dk

Abstract:

A hydraulic pitch-servo system is controlled using a nonlinear control law based on a port-controlled Hamiltonian formulation of the pitch-servo system. Not all systems can be formulated as port-controlled Hamiltonian systems, but hydraulic-mechanical systems similar to a pitch-servo system are well suited and control laws based on the presented method have previously been implemented with success. The method is implemented in a hydraulic-mechanic pitch-servo and blade model which takes effects of bend-twist couplings caused by large deformations into account.
Key words: pitch-servo system, port controlled hamiltonian systems with dissipation (PCHD), interconnection damping assignment - passivity-based control (IDA-PBC)

1 Introduction

Hydraulic pitch-servo systems are nonlinear in their physical behavior and control algorithms, that seek to control the pitch angle of the wind turbine blade actuated by a hydraulic pitch-servo, could benefit from taking the nonlinearities into account.

The system to be controlled can be described as a port-controlled Hamiltonian system with dissipation (PCHD). The reformulation of a system to a PCHD formulation can prove to be difficult and often impossible but if the formulation is possible it becomes possible to design a nonlinear control law that in many cases shows good robustness properties and good overall performance in a large operation range, where linear controllers might fall short due to the nonlinearities of the system.

Although advanced control methods applied to hydraulic-mechanical systems in general are not a novelty, the special field of pitch-servo systems for wind turbine blades have not been investigated as thoroughly. An investigation of a traditional proportional controller applied to a hydraulic pitch-servo for wind turbine blades have been presented in [1].

The wind turbine blade, which constitutes the mechanical part of the model, is modeled as being deformable and with bend-twist couplings [2]. The structural properties of the blade are based on the NREL 5MW Reference Wind Turbine [3].

PCHD-based control algorithms have already been implemented on hydraulic-mechanical systems similar to the pitch-servo system of a wind turbine blade [4]. Only the rotational symmetric inertial mass is however included in the PCHD formulation. Thus blade deformability and bend-twist couplings act as disturbances on an otherwise rotational symmetric inertial mass, which the blade can be considered to be.

The novelty of the work presented is in this paper is the specific application of the controller on pitch-servo systems with deformable blades and the implications of the disturbances occurring from the fact the controlled blade model is more complex than assumed by the controller.

The paper is organized in the following manner: Hydraulic and structural blade models are presented in the first section. Next the control methods are explained. Thereafter, control methods are tested through simulation on the combined blade and hydraulic model and the results are discussed.

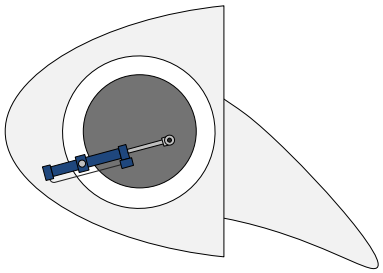

Figure 1: The hydraulic pitch-servo in a wind turbine rotor hub.

2 Models

In this section the different sub models and their interconnection is introduced.

2.1 Hydraulic Piston

The volumetric flows $Q_{a,b}$ through a four way spool valve can be described by a linear relationship between the nominal volumetric flows $\Xi_{a,b}$ and the valve spool displacement x_v

$$Q_i(P_i, x_v) = x_v \Xi_i(P_i, \text{sign}(x_v)), \quad i = a, b \quad (1)$$

where

$$\begin{aligned}
\Xi_a(P_a, \text{sign}(x_v)) &= k_v\sqrt{P_s - P_a}, && \text{for } x_v \geq 0 \\
\Xi_b(P_b, \text{sign}(x_v)) &= -k_v\sqrt{P_b - P_t}, && \text{for } x_v \geq 0 \\
\Xi_a(P_a, \text{sign}(x_v)) &= k_v\sqrt{P_a - P_t}, && \text{for } x_v < 0 \\
\Xi_b(P_b, \text{sign}(x_v)) &= -k_v\sqrt{P_s - P_b}, && \text{for } x_v < 0
\end{aligned}$$

and k_v is the valve coefficient, $P_{a,b}$ are the pressures of the two hydraulic chambers in the piston cylinder, P_s and P_t are the supply and tank pressure of the, respectively. The rates of change of pressure in the two hydraulic chambers are given by

$$\dot{P}_a = \frac{\beta_e}{V_a}(Q_a - A_a v_h) \quad (2a)$$

$$\dot{P}_b = \frac{\beta_e}{V_b}(Q_b + A_b v_h) \quad (2b)$$

which can be derived from the mass continuity equation for a control volume (cv) $\dot{m}_{cv} = \dot{m}_{in} - \dot{m}_{out}$ and the bulk modulus $\beta_e = -V\frac{\partial P}{\partial V}$ of a compressible fluid.

The resulting force of the hydraulic piston is

$$F_h = A_a P_a - A_b P_b \quad (3)$$

where $A_{a,b}$ are the areas of the piston in the two hydraulic chambers.

2.2 Structural Blade Model

The blade model [2] has been linearized at a wind speed of 12 m/s assuming nominal rotational speed of the rotor and steady state deformation of the blade due to aerodynamic loading. No aerodynamic damping have however been included in the model.

2.2.1 1 Degree of Freedom

In this simplified model, only the blade pitch DOF θ have been included. The blade is assumed rotational symmetric, rigid with a moment of inertia m and a damping d

$$\begin{bmatrix}\dot{\theta} \\ \ddot{\theta}\end{bmatrix} = \begin{bmatrix}0 & 1 \\ 0 & -\frac{d}{m}\end{bmatrix}\begin{bmatrix}\theta \\ \dot{\theta}\end{bmatrix} + \begin{bmatrix}0 \\ \frac{1}{m}\end{bmatrix} T \quad (4)$$

The blade is affected by the resulting torque $T = T_h + T_l$, where T_h is the torque exerted at blade the blade root by the pitch-servo and T_l is the external loading torque stemming from e.g. aerodynamic loading.

2.2.2 4 Degrees of Freedom

The 4 DOF blade model includes, apart from the pitch θ, also the edgewise q_e, flapwise q_f and torsional q_t displacements of the blade w.r.t. the steady state deformed blade. The coordinates of the blade model are given as

$$\boldsymbol{q} = [q_e \; q_f \; q_t \; \theta]^T$$

The governing equations of the structural blade model are given by

$$\mathbf{M}\ddot{\boldsymbol{q}} + [\mathbf{G} + \mathbf{C}]\dot{\boldsymbol{q}} + \mathbf{K}\boldsymbol{q} = \mathbf{F}, \; \mathbf{F} = [0\;0\;0\;T]^T \quad (5)$$

where the matrices $\mathbf{M}$, $\mathbf{G}$, and $\mathbf{K}$ are the mass, gyroscopic and stiffness matrices respectively. The moment of inertia of the 1 DOF model is given by $m = M_{44}$. The damping matrix $\mathbf{C}$ is not given by the model but have been chosen to be a diagonal matrix where $C_{ii} = 2\zeta_i\sqrt{K_{ii}M_{ii}}$ for $i = 1, 2, 3$ where $\zeta = [\frac{0.02}{2\pi} \; \frac{0.02}{2\pi} \; \frac{0.04}{2\pi}]^T$ and $C_{44} = d$. This gives a blade model with the damped frequencies 1.06 Hz, 0.72 Hz, 8.10 Hz, of the first 3 DOF respectively.

The pitch DOF has a stable and an unstable pole. The instability comes from the fact that the blade is not rotational symmetric and if the deformed blade is pitched the loading forces will be change.

2.3 Geometric Interconnection

The blade root and the hydraulic piston are connected as shown in figure 2.

$$x_h = \sqrt{L^2 + r^2 - 2Lr\sin(\phi - \theta)} - l \quad (6)$$

The piston velocity is given by $v_h = \frac{dx_h}{d\theta}\dot{\theta}$. The torque applied by the hydraulic piston force on the blade root is $T_h = \frac{dx_h}{d\theta}F_h$. The external loading force given by the external loading torque is $F_l = (\frac{dx_h}{d\theta})^{-1}T_l$.

In this paper the geometric length l is identical to the piston chamber length l. The two lengths

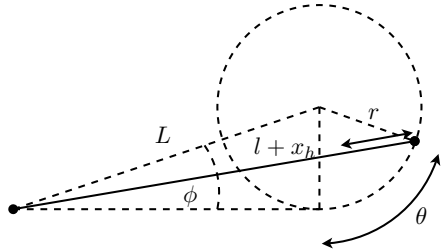

Figure 2: Geometry of pitch actuator mechanics.

could however be different in order to obtain a geometric interconnection similar to the one seen in Figure 1 where the rotation of the piston is not centered at the end of the piston but somewhere in the middle of the piston.

3 Control Methodologies

In this section the two different control methodoligies are presented. The two types of controllers are tuned with their control parameters to give a similar response when tracking a reference.

3.1 IDA-PBC of a PCHD

Interconnection damping assignment and passivity-based control (IDA-PBC) of a port-controlled Hamiltonian system with dissipation (PCHD) is presented in this section. As mentioned in the introduction of this paper, this heavily inspired by [4]. The resulting control laws are identical but they are constructed using different Hamiltonians and different interconnection assignment matrices. The disturbance observer used in [4] is also different from the one presented in this paper.

3.1.1 Port-controlled Hamiltonian system with Dissipation

A port-controlled Hamiltonian system with dissipation can be formulated as [5]

$$\dot{\boldsymbol{x}} = [\mathcal{J} - \mathcal{R}]\nabla\mathcal{H} + \mathcal{G}\boldsymbol{u} \tag{7a}$$

$$\boldsymbol{y} = \mathcal{G}^T\nabla\mathcal{H} \tag{7b}$$

where the Hamiltonian $\mathcal{H}$ is traditionally the sum of potential and kinetic energy in the system. The input and output port vectors are denoted $\boldsymbol{u}$ and $\boldsymbol{y}$, respectively. The matrices $\mathcal{J}$, $\mathcal{R}$ and $\mathcal{G}$ are called the interconnection, dissipation and port matrix, respectively. All of the matrices and the Hamiltonian are functions of the system state variable $\boldsymbol{x}$ but the functional argument notation $\boldsymbol{f}(\boldsymbol{x})$ has been omitted to ease notation, instead $\boldsymbol{f}$ is used and the reader is expected to include the functional argument on his own, when applicable. The differential operator ∇ indicates $\nabla\boldsymbol{f} = [\frac{d\boldsymbol{f}}{dx_1} \ \dots \ \frac{d\boldsymbol{f}}{dx_n}]^T$. The following definition is introduced to ease notation

$$\mathcal{F} \equiv \mathcal{J} - \mathcal{R}$$

The power conservation property of PCHD systems is described by the power-balance equation

$$\dot{\mathcal{H}} = \boldsymbol{u}^T\boldsymbol{y} - (\nabla\mathcal{H})^T\mathcal{R}\nabla\mathcal{H}$$

A Casimir function $\mathcal{C}$ w.r.t. $\mathcal{F}$ is a function which is the solution of the following PDE

$$(\nabla\mathcal{C})^T\mathcal{F} = 0 \tag{8}$$

and is dynamic invariant when there is no input to the system

$$\dot{\mathcal{C}} = 0 \text{ for } \boldsymbol{u} = 0 \tag{9}$$

this is a usefull tool to transform the coordinates of the system as seen in the next section.

3.1.2 Application to the Pitch-Servo

The 1DOF blade-pitch-servo system has the coordinates $\boldsymbol{x} = [q \ p \ P_a \ P_b]^T$ where the generalized position and momentum coordinates are $q = \theta$ and $p = \dot{\theta}m$, respectively.

The mechanical subsystem (q, p) has the Hamiltonian $\mathcal{H}_m = \mathcal{K}_m + \mathcal{V}_m$ where $\mathcal{K}_m = \frac{1}{2}\frac{p^2}{m}$ is the kinectic and $\mathcal{V}_m$ is the potential energy of the system.

If the servo-valve is closed, i.e. $x_v = 0$, the hydraulic subsystem (P_a, P_b) will act as nonlinear spring with the potential energy and thus Hamiltonian

$$\mathcal{H}_h = \int_{x_h^*}^{x_h} F_h dx_h \tag{10}$$

where x_h^* is the equilibrium point. The Hamiltonian of the total system is $\mathcal{H} = \mathcal{H}_m + \mathcal{H}_h$. The open-loop system has the combined interconnection and dissipation matrix and port matrix

$$\mathcal{F} = \begin{bmatrix} 0 & 1 & 0 & 0 \\ -1 & -d & \alpha_a & -\alpha_b \\ 0 & -\alpha_a & 0 & 0 \\ 0 & \alpha_b & 0 & 0 \end{bmatrix}, \ \mathcal{G} = \begin{bmatrix} 0 & 0 \\ 0 & 0 \\ \frac{\beta_e}{V_a} & 0 \\ 0 & \frac{\beta_e}{V_b} \end{bmatrix}$$

where $\alpha_i = \beta_e\frac{A_i}{V_i}$, for $i = a, b$. The port matrix of the system is $\boldsymbol{u} = [Q_a \ Q_b]^T = [\Xi_a \ \Xi_b]^T x_v$.

The combined interconnection and dissipation matrix $\mathcal{F}$ has rank of 2 which suggest that a coordinate transformation to canonical coordinates is possible. Such a transformation might ease the synthesis of an appropiate control law. The existence of dynamic invariant functions enables the transformation. Two functions which are solutions to (8) and thus dynamic invariant are

$$z_{ha} = A_a P_a + A_a \beta_e \ln\left(\frac{V_a}{V_{a0}}\right)$$
$$z_{hb} = A_b P_b + A_b \beta_e \ln\left(\frac{V_b}{V_{b0}}\right)$$

The difference between the two functions give another Casimir function

$$z_h = F_h + A_a \beta_e \ln\left(\frac{V_a}{V_{a0}}\right) - A_b \beta_e \ln\left(\frac{V_b}{V_{b0}}\right) \quad (11)$$

this gives inspiration to a coordinate transformation and the new coordinates are $\boldsymbol{x} = [q\ p\ z_h]^T$ with the combined interconnection and dissipation matrix and port matrix

$$\mathcal{F} = \begin{bmatrix} 0 & 1 & 0 \\ -1 & -d & 0 \\ 0 & 0 & 0 \end{bmatrix},\ \mathcal{G} = \begin{bmatrix} 0 \\ 0 \\ 1 \end{bmatrix}$$

and the input $\boldsymbol{u} = \left(\frac{\beta_e A_a}{V_a}\Xi_a - \frac{\beta_e A_b}{V_b}\Xi_b\right) x_v$.

Next a controller using interconnection and damping assignment passivity-based control is to be designed. The aim is to shape the desired Hamiltonian of the closed-loop system by assigning an additional Hamiltonian to the original system $\mathcal{H}_d = \mathcal{H} + \mathcal{H}_a$ such that $\mathcal{H}_d$ has a minimum at q_d^* given by the set

$$\left\{\boldsymbol{x}_d^* \in \mathcal{X} | p_d^* = 0,\ A_a P_{a,d}^* - A_b P_{b,d}^* = -F_l\right\} \quad (12)$$

where the loading force is the sum of the conservative and nonconservative forces acting on the system $F_l = \nabla_q \mathcal{V}_{m,d} + F_{ex}$. The desired Hamiltonian for the hydraulic system is

$$\mathcal{H}_{h,d} = \int_{x_{h,d}^*}^{x_h} F_h dx_h \quad (13)$$

giving a desired Hamiltonian for the total system $\mathcal{H}_d = \mathcal{H}_{f,d} + \mathcal{V}_{m,d} + \mathcal{K}_m$. The desired combined interconnection and dissipation matrix, which is obtained by assigning an additional interconnection and dissipation matrix $\mathcal{F}_d = \mathcal{F} + \mathcal{F}_a$, is

$$\mathcal{F}_d = \begin{bmatrix} 0 & 1 & -k_p \\ -1 & -d & k_d \\ k_p & -k_d & 0 \end{bmatrix}$$

The control law is given by [6]

$$\boldsymbol{u} = [\mathcal{G}^T \mathcal{G}]^{-1} \mathcal{G}^T [\mathcal{F}_d \nabla \mathcal{H}_a + \mathcal{F}_a \nabla \mathcal{H}] \quad (14)$$

where $\mathcal{H}_a$ is the solution the PDE

$$\mathcal{G}^\perp \mathcal{F}_d \nabla \mathcal{H}_a = \mathcal{G}^\perp \mathcal{F}_a \nabla \mathcal{H}$$

and where $\mathcal{G}^\perp$ is the left annihilator of $\mathcal{G}$, i.e. $\mathcal{G}^\perp \mathcal{G} = 0$.

The control law is finally seen the be

$$\boldsymbol{u} = -k_p \bar{z}_h - k_d v_h, \quad \bar{z}_h = z_h - z_{h,d}^* \quad (15)$$
$$x_v = \left(\frac{\beta_e A_a}{V_a}\Xi_a - \frac{\beta_e A_b}{V_b}\Xi_b\right)^{-1} \boldsymbol{u} \quad (16)$$

The control law requires accurate knowledge of $F_{h,d}^* = -F_l$ as seen by (12) which might not be possible due to external disturbances and modelling errors. A disturbance observer is constructed to estimate the unknown disturbance F_l. The observer coordinates are $\boldsymbol{\xi} = [q\ p\ T_l]^T$, $\boldsymbol{y}_\xi = [q\ \dot{q}]^T$, $\boldsymbol{u}_\xi = T_h$ with the system matrices

$$\mathbf{A} = \begin{bmatrix} 0 & 1 & 0 \\ 0 & -\frac{d}{m} & 1 \\ 0 & 0 & 0 \end{bmatrix}, \quad \mathbf{B} = \begin{bmatrix} 0 \\ \frac{1}{m} \\ 0 \end{bmatrix}, \quad \mathbf{C} = \begin{bmatrix} 1 & 0 & 0 \\ 0 & \frac{1}{m} & 0 \end{bmatrix}$$

If the velocity measurement is not available, the second rows of $\mathbf{y}_\xi$ and $\mathbf{C}$ should be omitted. The observer dynamics are given by

$$\dot{\hat{\boldsymbol{\xi}}} = \mathbf{A}\hat{\boldsymbol{\xi}} + \mathbf{B}\boldsymbol{u}_\xi + \mathbf{L}[\boldsymbol{y}_\xi - \mathbf{C}\hat{\boldsymbol{\xi}}] \quad (17)$$

where the observer gain $\mathbf{L}$ can be determined by the continuous time algebraic Ricatti equation, if the observer is linear quadratic in its penalty of the estimation errors $\boldsymbol{e} = \hat{\boldsymbol{\xi}} - \boldsymbol{\xi}$,

$$\mathbf{LCP} = \mathbf{AP} + \mathbf{PA}^T + \mathbf{Q},\ \mathbf{L} = \mathbf{PC}^T\mathbf{R}^{-1}$$

the estimation error weights are tuned by three parameters r_x, r_d and r_y

$$\mathbf{Q} = \begin{bmatrix} r_x^2 & 0 & 0 \\ 0 & r_x^2 & 0 \\ 0 & 0 & r_d^2 \end{bmatrix}, \quad \mathbf{R} = \begin{bmatrix} r_y^2 & 0 \\ 0 & r_y^2 \end{bmatrix}$$

It could be noted that the Hamiltonian of the observer is $\mathcal{H}_o = \frac{1}{2}\boldsymbol{e}^T\mathbf{P}\boldsymbol{e}$. No further analysis of the observer will however be performed and the reader is asked to see [4] for a detailed analysis of a similar, but not identical, observer.

3.2 Proportial-derivative Controller

A proportinal-derivative controller is given by

$$x_v = -(k_d s + k_p)\bar{x}_h = -k_p \bar{x}_h - k_d v_h \quad (18)$$

where $\bar{x}_h = x_h(\theta) - x_h(\theta_d)$ and s is the Laplace domain variable.

If no velocity measurement is available the controller is implemented as a lead compensator to reduce noise amplification.

$$x_v = -\frac{k_d s + k_p}{\alpha \frac{k_d}{k_p} s + 1} \bar{x}_h, \quad \alpha < 1 \tag{19}$$

The difference between the PD controller and the lead compensator is the addition of a low pass filter with a cut off frequency $f_\alpha = \frac{k_d}{2\pi k_p \alpha}$ Hz.

4 Results

Simulations have been carried out with both the 1 DOF and the 4 DOF blade model. Figures 3 and 4 on page 6 show the results for the two cases, respectively.

In both cases 4 different controllers have been created and tested: IDA-PBC and the lead compensator which does not have a velocity measurement. The IDA-PBC v and the PD controller which both utilize a velocity measurement.

A constant steady state torque of 1.68 kNm is applied to the blade acting as a external disturbance. Additional disturbance torques are added to the steady state torque and the resulting disturbance torque T_l can be seen in Figure 6.

The controllers are all tuned to have similar a reference tracing response as seen in Figures 3(a) and 4(a). The disturbances are also successfully rejected by all of the controllers as seen in the before mentioned figures. The IDA-PBC(v) controllers display better damping properties than the PD/lead controllers when as seen when zoomed in as in Figures 3(b), 4(b), 3(c), 4(c), 3(d) and 4(d).

The 3 extra DOF from the 4 DOF blade model are shown in Figure 5. The generalized coordinates have been translated to the corresponding coordinates in the blade tip. It can be seen that the edgewise and torsional DOF are coupled which also couples to the pitch DOF as seen in the estimated loading forces T_l in Figure 6.

Figure 6 shows, as just mentioned, the loading forces estimated by the IDA-PBC (v) observer. The observer for the 1 DOF simulations estimates $\hat{F}_h^*$ to be $-F_l$ whereas in the 4 DOF simulations the bend-twist coupling etc. have a much larger influence than the external loading. Furthermore the steady state loading forces have an offset w.r.t. regards to the actual external loading force this is caused by the unstable pole in the 4 DOF blade model as mentioned in section 2.2.2.

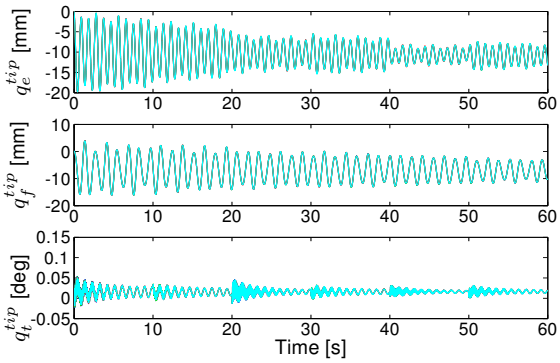

Figure 5: 4DOF: (–) Lead (–) PD (–) IDA-PBC (–) IDA-PBC v

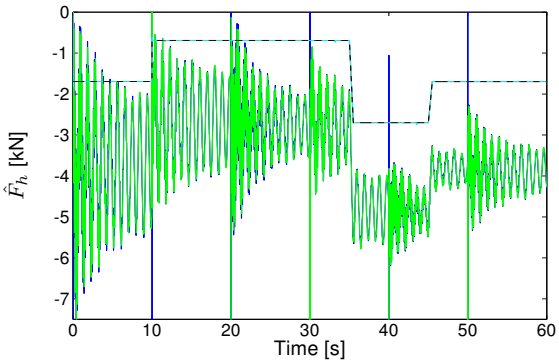

Figure 6: IDA-PBC (v): (–) 4 DOF (v) (–) 4 DOF (–) 1 DOF (v) (–) 1 DOF (–) T_l

5 Conclusion

The two control methods have been tested on both a 1 DOF and a 4 DOF linearized blade model and the IDA-PBC achieves better damping than the lead compensator when both methods are tuned to give a similar response

The IDA-PBC offers a nonlinear control method suited for the non-linearity of hydraulic dynamics in the pitch-servo system. The method does however require knowledge of the pressure in the two hydraulic chamber to calculate the hydraulic force and thus estimate the external loading force exerted on the pitch-servo system. If pressure measurements are not available, the short coming could perhaps be remedied by an estimate of the pressures via a modification of the implemented observer.

It is expected that the PD/lead controllers would show better damping if a feedback from the pressures of the hydraulic chambers where somehow implemented in the controllers. This has however not been explored in this paper.

Some of the physical parameters used in this paper have been chosen rather arbitrarily e.g. are the surface areas of the hydraulic piston are rather

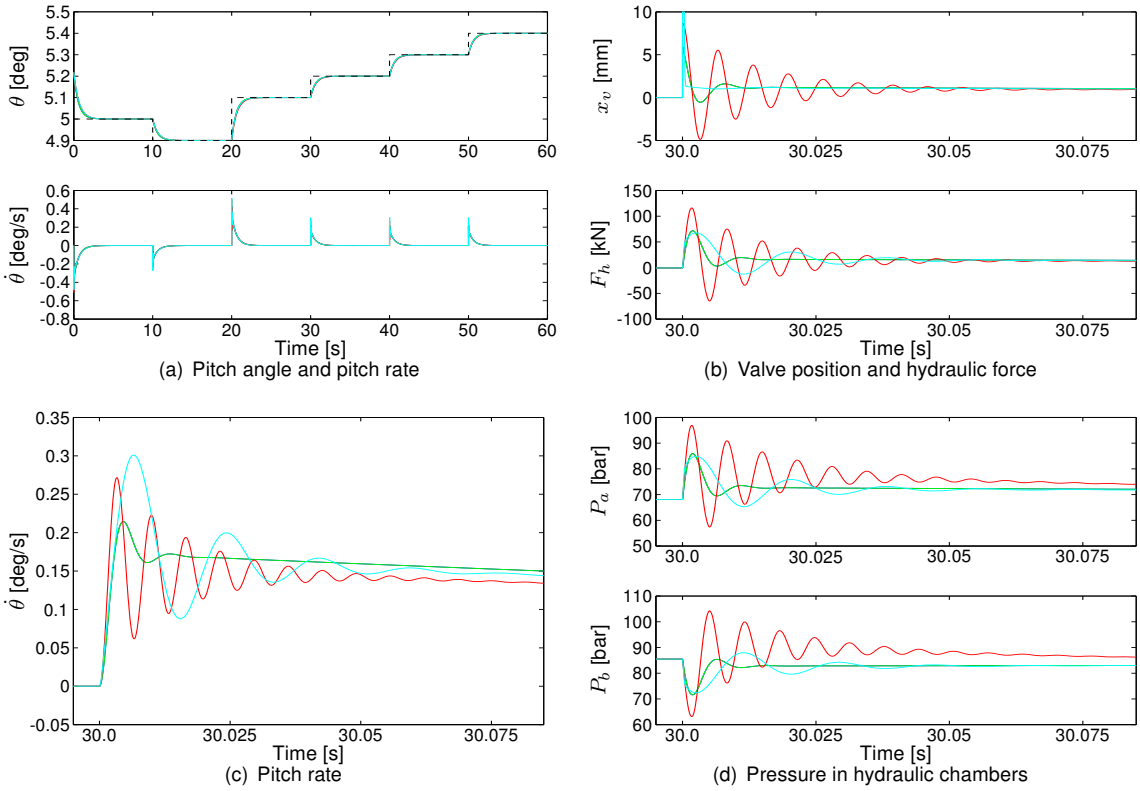

Figure 3: 1DOF: (–) IDA-PBC v (–) IDA-PBC (–) PD (–) Lead

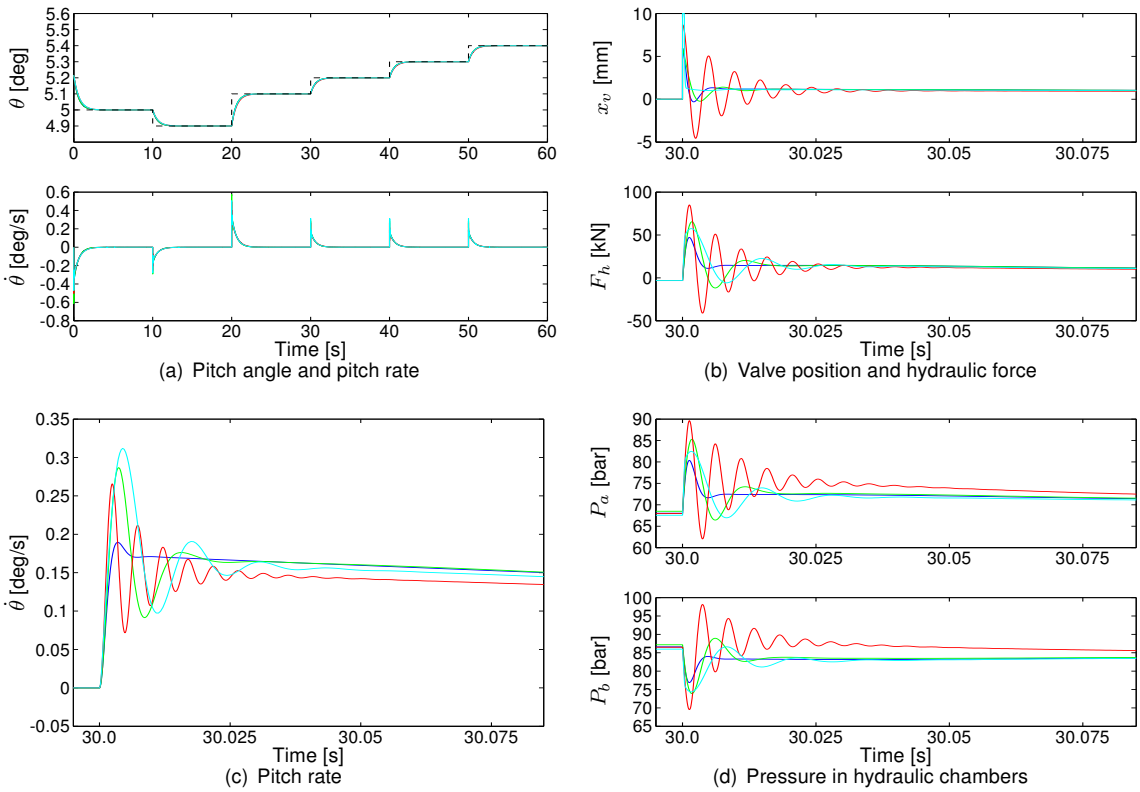

Figure 4: 4DOF: (–) IDA-PBC v (–) IDA-PBC (–) PD (–) Lead

large but the conclusions and results w.r.t to the controllers are expected to be valid also for a more realistic dimensioning of the pitch-servo system.

6 Acknowledgments

I wish to thank M. H. Hansen from Risø DTU and M. B. Larsen from DTU Electrical Engineering for their assistance and discussions regarding implementation of respectively blade model and control algorithm. The work presented in this paper is part of my Ph.D. study which is funded by Risø National Laboratory for Sustainable Energy, Technical University of Denmark.

References

[1] M. H. Hansen and B. S. Kallesøe. Servo-elastic dynamics of a hydraulic actuator pitching a blade with large deflections. *Journal of Physics: Conference Series*, 75(1):012077, 2007.

[2] B. S. Kallesøe. Equations of motion for a rotor blade, including gravity, pitch action and rotor speed variations. *Wind Energy*, 10(3):209–230, 2007.

[3] J. Jonkman, S. Butterfield, W. Musial, and G. Scott. Definition of a 5-mw reference wind turbine for offshore system development. Technical report, NREL/NWTC, 2007.

[4] G. Grabmair and K. Schlacher. Energy-based nonlinear control of hydraulically actuated mechanical systems. In *Proceedings of the 44th IEEE Conference on Decision and Control*, pages 7520–7525, 2005. ISBN 0780395670.

[5] A. van der Schaft. *L2-gain and Passivity Techniques in Nonlinear Control*. Springer, 2000.

[6] Romeo Ortega, Arjan van der Schaft, Bernhard Maschke, and Gerardo Escobar. Interconnection and damping assignment passivity-based control of port-controlled hamiltonian systems. *Automatica*, 38(4): 585–596, 2002.

A Parameters of plant and controller tuning

The following physical parameters have been chosen A_a = 0.025 m^{2}and A_b = 0.02 m^2. $V_{a0,b0}$ = 0.05 A_a m^3. P_s = 2e7 Pa and P_t = 1e5 Pa. k_v = 1e-3 m^{3}s^{-1} Pa$^{-1/2}$ mm^{-1} and β_e = 1.6e9 Pa. $|x_{v,abs}|$ = 1 mm.

The linearized matrices for the 4 DOF blade model are

$$\mathbf{M} = 1\mathrm{e}4 \begin{bmatrix} 0.1464 & 0 & -0.0016 & -0.4480 \\ 0 & 0.0785 & -0.0228 & 0.0056 \\ -0.0016 & -0.0228 & 0.0567 & 0.1949 \\ -0.4480 & 0.0056 & 0.1949 & 4.5823 \end{bmatrix}$$

$$\mathbf{K} = 1\mathrm{e}6 \begin{bmatrix} 0.0648 & -0.0038 & 0.0361 & 0.0071 \\ -0.0038 & 0.0167 & -0.0047 & 0.0008 \\ 0.0360 & -0.0066 & 1.2830 & -0.0003 \\ 0.0071 & 0.0053 & 0.0011 & -0.0219 \end{bmatrix}$$

$$\mathbf{C} = 1\mathrm{e}6 \begin{bmatrix} 0.0001 & 0 & 0 & 0 \\ 0 & 0.0000 & 0 & 0 \\ 0 & 0 & 0.0003 & 0 \\ 0 & 0 & 0 & 5.7296 \end{bmatrix}$$

$$\mathbf{G} = \begin{bmatrix} 0 & 0 & 0 & -56.6019 \\ 0 & 0 & 0 & 3.5808 \\ 0 & 0 & 0 & 0 \\ 0 & 0 & 0 & 0 \end{bmatrix}$$

The geomtric parameters are chosen to be L = 2.3 m, l = 1.5 m and r = 1 m.

The control parameters for the IDA-PBC controller are k_p = 500, k_d = 0.2 β_e, r_x = 1e-6, r_d = 1e6 and r_y = 1e-6.

The control parameters for the lead compensator are k_p = 0.75, k_d = 0.05 and α = 0.001.

The control parameters for the PD controller are k_p = 5 and k_d = 0.05.